Bayesian Analysis (2014) **9**, Number 3, pp. 521–550

Robust Bayesian Graphical Modeling Using Dirichlet t-Distributions

Michael Finegold [*] and Mathias Drton [†]

Abstract. Bayesian graphical modeling provides an appealing way to obtain uncertainty estimates when inferring network structures, and much recent progress has been made for Gaussian models. For more robust inferences, it is natural to consider extensions to t-distribution models. We argue that the classical multivariate t-distribution, defined using a single latent Gamma random variable to rescale a Gaussian random vector, is of little use in more highly multivariate settings, and propose other, more flexible t-distributions. Using an independent Gamma-divisor for each component of the random vector defines what we term the alternative t-distribution. The associated model allows one to extract information from highly multivariate data even when most experiments contain outliers for some of their measurements. However, the use of this alternative model comes at increased computational cost and imposes constraints on the achievable correlation structures, raising the need for a compromise between the classical and alternative models. To this end we propose the use of Dirichlet processes for adaptive clustering of the latent Gamma-scalars, each of which may then divide a group of latent Gaussian variables. The resulting Dirichlet t-distribution interpolates naturally between the two extreme cases of the classical and alternative t-distributions and combines more appealing modeling of the multivariate dependence structure with favorable computational properties.

Keywords: Bayesian inference, Dirichlet process, graphical model, Markov chain Monte Carlo, t-distribution.

1 Introduction

Consider a random vector $\mathbf{Y} = (Y_1, \ldots, Y_p)$ and an undirected graph $G = (V, E)$ with vertex set $V = \{1, \ldots, p\}$. The Gaussian graphical model given by the graph G assumes that $\mathbf{Y}$ follows a multivariate normal distribution $\mathcal{N}_p(\boldsymbol{\mu}, \boldsymbol{\Sigma})$, where $\boldsymbol{\mu}$ may be any mean vector in $\mathbb{R}^p$ but $\boldsymbol{\Sigma}$ is a positive definite covariance matrix that is constrained such that two variables Y_j and Y_k are conditionally independent given all the remaining variables $\mathbf{Y}_{\setminus\{j,k\}}$ whenever $\{j, k\}$ is not an edge in E. The conditional independence holds if and only if $\Sigma^{-1}_{jk} = 0$; see e.g. Lauritzen (1996). Hence, the graph of a Gaussian graphical model can be inferred from data by inferring the pattern of non-zero entries in the precision matrix $\boldsymbol{\Sigma}^{-1}$.

Different Bayesian methods have been developed for an uncertainty assessment in inference of the graph. Giudici and Green (1999), for instance, use a uniform prior on decomposable graphs and place a Hyper Inverse Wishart prior on the covariance matrix,

[*] Dept. of Statistics, Carnegie Mellon University, Pittsburgh, PA, U.S.A. mfinegol@andrew.cmu.edu
[†] Dept. of Statistics, University of Washington, Seattle, WA, U.S.A. md5@uw.edu

DOI:10.1214/13-BA856

which allows for exact local computation (Dawid and Lauritzen 1993). In particular, a closed form marginal likelihood permits treatment of high-dimensional datasets (Dobra et al. 2004; Jones et al. 2005). Exact computations for non-decomposable graphs are much more involved (Roverato 2002; Dellaportas et al. 2003; Atay-Kayis and Massam 2005); for an approximate treatment see Lenkoski and Dobra (2011). Other recent literature providing different extensions to the basic Gaussian model includes Rajaratnam et al. (2008) and Carvalho and Scott (2009).

While appealing in many respects, Gaussian methods are susceptible to measurement errors. There is a substantial literature on robustness in Bayesian inference, including De Finetti (1961) and West (1984), but less work that directly targets graphical models. One commonly taken approach replaces multivariate normal by multivariate t-distributions (with univariate t-margins). T-distributions yield reasonable models for heavy-tailed marginal behavior and have the capacity to maintain good statistical efficiency when data are in fact Gaussian. Moreover, convenient closed form conditional distributions are available for use in Markov chain Monte Carlo algorithms that exploit the representation of t-random variables as ratios involving Gaussian and Gamma random variables.

The classical multivariate t-distribution can be defined in terms of an unobserved Gaussian random vector and a single unobserved Gamma divisor. In the context of this paper, modeling assumptions then refer to the latent Gaussian vector. Penalized likelihood techniques for graphical model selection with this classical t-distribution were explored in Yuan and Huang (2009). Highly multivariate data, however, often have pockets of contamination in many observations creating a scenario to which the classical t-distribution is poorly suited. This paper addresses this problem by developing methods based on more flexible t-distributions. The distribution we term the alternative t-distribution has independent Gamma scalars for each component of the latent Gaussian vector. This construction has been used in a frequentist treatment of graphical models (Finegold and Drton 2011), but seems to have received little attention otherwise. While better suited to higher-dimensional analysis, the distribution's use comes at increased computational cost and imposes constraints on the achievable correlation structures; see Figure 9 in Finegold and Drton (2011). It is thus desirable to achieve a trade-off between the two extremes, 'classical' versus 'alternative'.

The key new contribution of this paper is an adaptive method to interpolate between the classical and the alternative case. Our proposal uses Dirichlet processes to cluster the Gamma divisors associated with the components of the latent Gaussian vector. The common Gamma-value associated with a cluster is then used to divide all the associated Gaussian variables. The Dirichlet process clustering thus pertains to the possibly dependent components of a single multivariate observation, as opposed to the common case of clustering different independent observations. Compared to the alternative case, the Dirichlet t-proposal alleviates constraints on correlations and reduces computational effort when a small number of divisors is sufficient. While we are concerned with graphical models, there is no limitation to the use of the Dirichlet t-framework in other problems of multivariate statistics.

The paper is organized as follows. Section 2 lays out the Gaussian setup upon which our extensions are based. In Section 3, we describe Bayesian inference of network structures with classical and alternative t-distributions. The Dirichlet t-distribution is developed in Section 4. Numerical experiments (Section 5) and an analysis of gene expression data (Section 6) demonstrate that our new framework is computationally tractable and statistically efficient across a broad spectrum of data with outliers. Concluding remarks are given Section 7.

2 Bayesian Inference for Gaussian Graphical Models

2.1 Background

Let $IW_p(m, \boldsymbol{\Phi})$ denote the Inverse Wishart (IW) distribution with degrees of freedom $m > p-1$ and a positive definite scale matrix $\boldsymbol{\Phi}$. This distribution is supported on the cone of $p \times p$ positive definite matrices and has density

$$p(\boldsymbol{\Sigma} \mid m, \boldsymbol{\Phi}) = \frac{|\frac{\boldsymbol{\Phi}}{2}|^{\frac{m}{2}}}{\Gamma_p(\frac{m}{2})} |\boldsymbol{\Sigma}|^{-\frac{m+p+1}{2}} \exp\left\{-\frac{1}{2}\mathrm{tr}\left(\boldsymbol{\Phi}\boldsymbol{\Sigma}^{-1}\right)\right\}, \tag{1}$$

where the determinant of a matrix $\boldsymbol{A}$ is denoted $|\boldsymbol{A}|$ and

$$\Gamma_p(\alpha) = \pi^{p(p-1)/4} \prod_{i=1}^{p} \Gamma\left(\alpha - \left(\frac{i-1}{2}\right)\right)$$

is the multivariate gamma function with argument $\alpha > (p-1)/2$. The distribution is the conjugate prior for the covariance matrix of a multivariate normal distribution.

Let $G = (V, E)$ be a decomposable graph with vertex set $V = \{1, \ldots, p\}$, and suppose $C_1, S_2, C_2, \ldots, S_m, C_m$ is a perfect sequence of the graph's cliques C_i and separators S_i. Here and throughout the paper, we assume familiarity with basic graphical concepts as introduced in Lauritzen (1996). Let $M^+(G)$ be the set of positive definite matrices $\boldsymbol{\Sigma}$ with entry $\Sigma_{jk} = 0$ whenever $\{j, k\}$ is not an edge in E. For Gaussian graphical modeling, one needs a constrained version of the IW distribution for the covariance matrix $\boldsymbol{\Sigma}$ that has support such that the precision matrix $\boldsymbol{\Sigma}^{-1}$ lies in $M^+(G)$. The relevant distribution is known as the Hyper IW distribution and we denote it by $HIW(G, \delta, \boldsymbol{\Phi})$, where $\delta > 0$ is a degrees of freedom parameter and $\boldsymbol{\Phi}$ is a positive definite scale matrix. The distribution's density

$$f(\boldsymbol{\Sigma} \mid G, \delta, \boldsymbol{\Phi}) = \frac{\prod_{i=1}^{m} p(\boldsymbol{\Sigma}_{C_iC_i} \mid \delta + |C_i| - 1, \boldsymbol{\Phi}_{C_iC_i})}{\prod_{i=2}^{m} p(\boldsymbol{\Sigma}_{S_iS_i} \mid \delta + |S_i| - 1, \boldsymbol{\Phi}_{S_iS_i})}$$

is the ratio of products of evaluations of the IW density from (1). Here, $\boldsymbol{\Sigma}_{AA}$ and $\boldsymbol{\Phi}_{AA}$ denote the principal submatrices indexed by a set $A \subset \{1, \ldots, p\}$. It follows from properties of the IW distribution that the normalizing constant for the HIW distribution is:

$$h(G,\delta,\mathbf{\Phi}) = \frac{\prod_{i=1}^{m} \left|\frac{\mathbf{\Phi}_{C_iC_i}}{2}\right|^{(\delta+|C_i|-1)/2} \Gamma_{|C_i|}\left(\frac{\delta+|C_i|-1}{2}\right)^{-1}}{\prod_{i=2}^{m} \left|\frac{\mathbf{\Phi}_{S_iS_i}}{2}\right|^{(\delta+|S_i|-1)/2} \Gamma_{|S_i|}\left(\frac{\delta+|S_i|-1}{2}\right)^{-1}}. \tag{2}$$

The HIW distribution has the consistency property that the clique submatrix distribution $P(\mathbf{\Sigma}_{C_iC_i} \mid G, \delta, \mathbf{\Phi})$ is the same for any graph G with clique C_i (Dawid and Lauritzen 1993).

2.2 Model and Prior Specification

We will treat a particular setup for Bayesian inference in Gaussian graphical models that is similar to models in work such as Armstrong et al. (2009). The considered prior on graphs, $P(G)$, is supported on the set of decomposable graphs with the probabilities of graphs proportional to

$$d^{|E|}(1-d)^{\binom{p}{2}-|E|}. \tag{3}$$

The parameter d controls the sparsity of the graph. Conditional on G and hyperparameters δ and $\mathbf{\Phi}$, we let the covariance matrix $\mathbf{\Sigma}$ follow a $HIW(G,\delta,\mathbf{\Phi})$ distribution. Larger δ makes the posterior more concentrated around the hyperparameter $\mathbf{\Phi}$. As in Carvalho and Scott (2009) and Donnet and Marin (2012), we choose $\delta = 1$. We use matrix hyperparameter $\mathbf{\Phi} = c\boldsymbol{\mathcal{I}}_p$, a scalar multiple of the $p \times p$ identity matrix. Larger c leads to larger graphs; see Jones et al. (2005).

Finally, suppose we observe a sample of n independent random vectors $\mathbf{Y}_1, \ldots, \mathbf{Y}_n$ drawn from $\mathcal{N}_p(\mathbf{0}, \mathbf{\Sigma})$. Let $\mathbf{Y}$ be the matrix with the vectors $\mathbf{Y}_i$ as rows. The joint distribution of $(\mathbf{Y}, G, \mathbf{\Sigma})$ then factors as

$$P(\mathbf{Y}, G, \mathbf{\Sigma} \mid \delta, \mathbf{\Phi}) = P(G)P(\mathbf{\Sigma} \mid G, \delta, \mathbf{\Phi}) \prod_{i=1}^{n} P(\mathbf{Y}_i \mid \mathbf{\Sigma}).$$

Centering Gaussian data by subtracting off the sample mean and assuming mean $\boldsymbol{\mu} = \mathbf{0}$ is standard practice since the distribution theory is essentially unchanged.

2.3 Metropolis-Hastings Sampler

We now briefly review the posterior sampling scheme used in prior work such as Armstrong et al. (2009). Define the sample covariance matrix

$$\boldsymbol{S} = (s_{jk}) = \frac{1}{n}\sum_{i=1}^{n} \mathbf{Y}_i \mathbf{Y}_i^T,$$

and set $\mathbf{\Phi}^* = \mathbf{\Phi} + n\boldsymbol{S}$ and $\delta^* = \delta + n$. Then

$$(\mathbf{\Sigma} \,|\, \mathbf{Y}, \delta, \mathbf{\Phi}, G) \sim \mathit{HIW}(G, \delta^*, \mathbf{\Phi}^*) \tag{4}$$

and

$$P(\mathbf{Y} \,|\, \delta, \mathbf{\Phi}, G) = \frac{1}{(2\pi)^{np/2}} \cdot \frac{h(G, \delta, \mathbf{\Phi})}{h(G, \delta^*, \mathbf{\Phi}^*)}; \tag{5}$$

see Dawid and Lauritzen (1993) and Giudici and Green (1999).

Let $G = (V, E)$ and $G' = (V, E')$ be two decomposable graphs on $V = \{1, \dots, p\}$. Suppose that $C_1, S_2, C_2, \dots, S_m, C_m$ is a perfect sequence of the cliques and separators of G and that $\{j, k\} \in E$. If G' is equal to G except that the edge $\{j, k\}$ is removed, then the following three properties hold; see e.g. Armstrong et al. (2009). First, the edge $\{j, k\}$ is in a single clique C_q of G. Second, we have either $j \notin S_q$ or $k \notin S_q$. Third, suppose $k \notin S_q$, and let $C_{q_1} = C_q \setminus \{k\}$, $C_{q_2} = C_q \setminus \{j\}$ and $S_{q_2} = C_q \setminus \{j, k\}$. Then $C_1, S_2, \dots, S_q, C_{q_1}, S_{q_2}, C_{q_2}, S_{q+1}, \dots, S_m, C_m$ is a perfect ordering of all cliques and separators of G'. Let $\delta_2 = \delta + |S_{q_2}|$ and $\delta_2^* = \delta^* + |S_{q_2}|$. The above three observations can be used to show that the ratio of marginal likelihoods $P(\mathbf{Y} \,|\, G)/P(\mathbf{Y} \,|\, G')$ is

$$\frac{h(G, \delta, \mathbf{\Phi}) h(G', \delta^*, \mathbf{\Phi}^*)}{h(G, \delta^*, \mathbf{\Phi}^*) h(G', \delta, \mathbf{\Phi})} = \frac{\left|\mathbf{\Phi}_{ee|S_{q_2}}\right|^{\left(\frac{\delta_2+1}{2}\right)} \left|\mathbf{\Phi}^*_{jj|S_{q_2}} \mathbf{\Phi}^*_{kk|S_{q_2}}\right|^{\left(\frac{\delta_2^*}{2}\right)}}{\left|\mathbf{\Phi}^*_{ee|S_{q_2}}\right|^{\left(\frac{\delta_2^*+1}{2}\right)} \left|\mathbf{\Phi}_{jj|S_{q_2}} \mathbf{\Phi}_{kk|S_{q_2}}\right|^{\left(\frac{\delta_2}{2}\right)}} \times \frac{\Gamma\left(\frac{\delta_2}{2}\right) \Gamma\left(\frac{\delta_2^*+1}{2}\right)}{\Gamma\left(\frac{\delta_2+1}{2}\right) \Gamma\left(\frac{\delta_2^*}{2}\right)}. \tag{6}$$

Here, $e = \{j, k\}$ and $\mathbf{\Phi}_{ee|S_{q_2}} = \mathbf{\Phi}_{ee} - \mathbf{\Phi}_{eS_{q2}} (\mathbf{\Phi}_{S_{q2}S_{q2}})^{-1} \mathbf{\Phi}_{S_{q2}e}$; the conditional variances for j and k are defined similarly. The ratio in (6) allows one to create a Markov chain with the posterior distribution $P(G \,|\, \mathbf{Y})$ as the stationary distribution by applying a Metropolis-Hastings procedure that avoids sampling of $\mathbf{\Sigma}$.

Algorithm 1 (Gaussian)**.** *Starting with a decomposable graph G_0, repeat the following two steps for $t = 0, 1, 2, \dots$:*
(i) Create a graph G' by randomly picking an edge to delete from G_t or to add to G_t.
(ii) If G' is decomposable, accept the move $G_{t+1} = G'$ with probability

$$\min\left\{1, \frac{P(\mathbf{Y} \,|\, G')}{P(\mathbf{Y} \,|\, G)}\right\}, \tag{7}$$

setting $G_{t+1} = G$ if the move is rejected or G' is not decomposable.

Decomposability of the input G_0 can be tested with the Max-Cardinality algorithm (Cowell et al. 1999). Given the decomposable graph G_0, the set of all decomposable graphs can be traversed following simple rules for edge addition and deletion (Giudici and Green 1999).

3 Bayesian Graphical Modeling With t-Distributions

3.1 Classical and Alternative Multivariate t-Distributions

The *classical* multivariate t-distribution $t_{p,\nu}(\boldsymbol{\mu}, \boldsymbol{\Psi})$ in $\mathbb{R}^p$ has density

$$f_\nu(\mathbf{y} \,|\, \boldsymbol{\mu}, \boldsymbol{\Psi}) = \frac{\Gamma(\frac{\nu+p}{2})|\boldsymbol{\Psi}|^{-1/2}}{(\pi\nu)^{p/2}\Gamma(\frac{\nu}{2})[1 + \delta_y(\boldsymbol{\mu}, \boldsymbol{\Psi})/\nu]^{(\nu+p)/2}}, \tag{8}$$

where $\delta_y(\boldsymbol{\mu}, \boldsymbol{\Psi}) = (\mathbf{y} - \boldsymbol{\mu})^T \boldsymbol{\Psi}^{-1}(\mathbf{y} - \boldsymbol{\mu})$ and $\mathbf{y} \in \mathbb{R}^p$. The vector $\boldsymbol{\mu} \in \mathbb{R}^p$ is the mean vector. The scale parameter matrix $\boldsymbol{\Psi} = (\psi_{jk})$ is assumed positive definite. For degrees of freedom $\nu > 2$, the covariance matrix exists and is equal to $\nu/(\nu - 2)$ times $\boldsymbol{\Psi}$. If $\mathbf{X} \sim \mathcal{N}_p(\mathbf{0}, \boldsymbol{\Psi})$ is a multivariate normal random vector independent of the Gamma-random variable $\tau \sim \Gamma(\nu/2, \nu/2)$, then the random vector $\mathbf{Y} = \boldsymbol{\mu} + \mathbf{X}/\sqrt{\tau}$ has a $t_{p,\nu}(\boldsymbol{\mu}, \boldsymbol{\Psi})$-distribution (Kotz and Nadarajah 2004, Chap. 1). The heavy tails of the distribution are related to small values of the divisor τ.

Consider a sample of n independent observations $\mathbf{Y}_1, \ldots, \mathbf{Y}_n \in \mathbb{R}^p$. When working with the classical t-distribution there is a single Gamma-distributed divisor associated with each observation $\mathbf{Y}_i$, which allows for reweighting of all or none of the associated latent vector $\mathbf{X}_i$. Hence, the classical t-distribution is useful for robust inference primarily in scenarios in which only a handful of the n observations is contaminated; these can be weighted down in entirety and information is drawn mainly from remaining uncorrupted observations. When the dimension p is large, however, it is not uncommon for contamination to affect rather small parts of many observations. To handle such situations better we introduce p divisors for each independent observation $\mathbf{Y}_i$.

Returning to the setting of a single random vector taking values in $\mathbb{R}^p$, consider p independent divisors $\tau_1, \ldots, \tau_p \sim \Gamma(\nu/2, \nu/2)$. Assuming the divisors to be independent of $\mathbf{X} \sim \mathcal{N}_p(0, \boldsymbol{\Psi})$, we create the random vector $\mathbf{Y}$ with coordinates $Y_j = \mu_j + X_j/\sqrt{\tau_j}$ and define the *alternative* multivariate t-distribution to be the joint distribution of $\mathbf{Y}$. In symbols, $\mathbf{Y} \sim t^*_{p,\nu}(\boldsymbol{\mu}, \boldsymbol{\Psi})$. For robustified inference, the alternative t-distribution is appealing as it allows different rescaling of the different components of $\mathbf{Y}$.

3.2 Bayesian Inference With Classical t-Distributions

Suppose $\mathbf{Y}_1, \ldots, \mathbf{Y}_n \in \mathbb{R}^p$ are independent random vectors drawn from the classical multivariate t-distribution $t_{\nu,p}(\boldsymbol{\mu}, \boldsymbol{\Psi})$. Let $\mathbf{Y}$ be the matrix with the vectors $\mathbf{Y}_i$ as rows. We are interested in the posterior distribution on graphs, $P(G \,|\, \mathbf{Y})$, where the graph G corresponds to conditional independence constraints on the latent multivariate normal vectors $\mathbf{X}_i$, that is, an off-diagonal entry θ_{jk} of the matrix $\boldsymbol{\Theta} = \boldsymbol{\Psi}^{-1}$ is zero unless $\{j, k\}$ is an edge in G.

In the normal model we can center the data by subtracting off the sample mean and assume, without loss of generality, that $\boldsymbol{\mu} = \mathbf{0}$. For the t-model, robust estimation of both $\boldsymbol{\mu}$ and $\boldsymbol{\Psi}$ is desirable, and we thus include $\boldsymbol{\mu}$ in our setup. Let $\boldsymbol{\tau} = (\tau_1, \ldots, \tau_n)$ be the vector of unobserved Gamma-divisors for the n observations $\mathbf{Y}_i$. Proceeding as in the normal case, our full model factors the joint distribution of $\mathbf{Y}, \boldsymbol{\tau}, G, \boldsymbol{\Psi}, \boldsymbol{\mu}$ as

$$P(\mathbf{Y}, \boldsymbol{\tau}, G, \boldsymbol{\Psi}, \boldsymbol{\mu}) = P(G)P(\boldsymbol{\mu})P(\boldsymbol{\Psi} \,|\, G, \delta, \boldsymbol{\Phi}) \prod_{i=1}^{n} P(\mathbf{Y}_i \,|\, \tau_i, \boldsymbol{\Psi}, \boldsymbol{\mu}) P(\tau_i \,|\, \nu), \tag{9}$$

where the distribution of the observations is determined by

$$(\mathbf{Y}_i \,|\, \tau_i, \boldsymbol{\Psi}) \sim \mathcal{N}_p(\boldsymbol{\mu}, \boldsymbol{\Psi}/\tau_i), \qquad (\tau_i \,|\, \nu) \sim \Gamma(\nu/2, \nu/2), \tag{10}$$

and the prior distributions are

$$(\boldsymbol{\Psi} \,|\, G, \delta, \boldsymbol{\Phi}) \sim \mathit{HIW}(G, \delta, \boldsymbol{\Phi}), \qquad \boldsymbol{\mu} \sim \mathcal{N}_p(\mathbf{0}, \sigma_\mu \cdot \boldsymbol{\mathcal{I}}_p). \tag{11}$$

In later numerical work, we choose σ_μ large enough for the prior to be "flat" over a range of plausible values. Throughout the hyperparameters δ, $\boldsymbol{\Phi}$, and ν are fixed; recall Section 2.2.

Inference for the Gaussian case is simplified by integrating out the covariance matrix $\boldsymbol{\Sigma}$; recall (6). In the t-model, we may condition on τ and add/remove edges based on the ratio

$$\frac{P(\mathbf{Y} \,|\, G', \tau, \boldsymbol{\mu})}{P(\mathbf{Y} \,|\, G, \tau, \boldsymbol{\mu})} = \frac{h(G, \delta, \boldsymbol{\Phi}) h(G', \delta^*, \boldsymbol{\Phi}^*_\tau)}{h(G, \delta^*, \boldsymbol{\Phi}^*_\tau) h(G', \delta, \boldsymbol{\Phi})}, \tag{12}$$

where

$$\boldsymbol{S}_{\boldsymbol{\tau}\mathbf{YY}}(\boldsymbol{\mu}) = \frac{1}{n} \sum_{i=1}^{n} \tau_i (\mathbf{Y}_i - \boldsymbol{\mu})(\mathbf{Y}_i - \boldsymbol{\mu})^T \qquad \text{and} \qquad \boldsymbol{\Phi}^*_\tau = \boldsymbol{\Phi} + n\boldsymbol{S}_{\boldsymbol{\tau}\mathbf{YY}}(\boldsymbol{\mu}). \tag{13}$$

Drawing $\boldsymbol{\tau}$ given $G, \boldsymbol{\mu}$ and $\mathbf{Y}$ is difficult, however, and we resort to conditioning on $\boldsymbol{\Psi}$ and will implement a Gibbs sampler that alternates between drawing from the following conditional distributions

$$[1.] \;\; (G \,|\, \mathbf{Y}, \boldsymbol{\tau}, \boldsymbol{\mu}), \quad [2.] \;\; (\boldsymbol{\Psi} \,|\, \mathbf{Y}, \boldsymbol{\tau}, \boldsymbol{\mu}, G), \quad [3.] \;\; (\boldsymbol{\tau} \,|\, \mathbf{Y}, \boldsymbol{\mu}, \boldsymbol{\Psi}), \quad [4.] \;\; (\boldsymbol{\mu} \,|\, \mathbf{Y}, \boldsymbol{\tau}, \boldsymbol{\Psi}, G).$$

The steps [1.] and [2.] draw from the joint distribution of $(G, \boldsymbol{\Psi})$ conditional on the remaining quantities and thus represent grouping in the sense of Liu (2001, Section 6.7).

As mentioned above, step [1.] can be addressed via the ratio in (12). For step [2.], we use the method of Carvalho et al. (2007) to draw from

$$(\boldsymbol{\Psi} \,|\, \mathbf{Y}, G, \tau, \boldsymbol{\mu}) \sim \mathit{HIW}(G, \delta^*, \boldsymbol{\Phi}^*_\tau). \tag{14}$$

Their procedure first draws $\boldsymbol{\Psi}_{C_1C_1}$, cycles through the cliques of G to draw $\boldsymbol{\Psi}_{C_iC_i}$ given $\boldsymbol{\Psi}_{S_i,S_i}$, and then uses a standard completion algorithm to determine the values of $\boldsymbol{\Psi}$ not associated with any clique. Next, for step [3.], we have the conditional distribution

$$(\tau_i \,|\, \mathbf{Y}, \boldsymbol{\mu}, \boldsymbol{\Psi}) \sim \Gamma\left(\frac{\nu + p}{2}, \frac{\nu + \delta_{\mathbf{Y}_i}(\boldsymbol{\mu}, \boldsymbol{\Psi})}{2}\right); \tag{15}$$

compare Liu and Rubin (1995). This requires the matrix inverse $\boldsymbol{\Theta} = \boldsymbol{\Psi}^{-1}$. For decomposable graphs, the inversion can be done efficiently using the procedure of Dawid and Lauritzen (1993). That is, we compute

$$\boldsymbol{\Theta} = \sum_{i=1}^{m} (\boldsymbol{\Psi}_{C_iC_i})^{-1\,[0]} - \sum_{i=2}^{m} (\boldsymbol{\Psi}_{S_iS_i})^{-1\,[0]}, \tag{16}$$

where $(\boldsymbol{\Psi}_{C_iC_i})^{-1\,[0]}$ means that we take the $p \times p$ matrix of zeros and add in the elements of $(\boldsymbol{\Psi}_{C_iC_i})^{-1}$ in their appropriate places. This calculation only requires the elements ψ_{jk} of $\boldsymbol{\Psi}$ corresponding to edges $\{j,k\} \in E$. Therefore, for the purposes of obtaining $\boldsymbol{\Theta}$, we need not perform the completion step in the method of Carvalho et al. (2007). Moreover, every step in the generation and inversion of $\boldsymbol{\Psi}$ is based on local computations at the clique level.

Now, for the final step [4.], the conditional distribution $(\boldsymbol{\mu} \,|\, \mathbf{Y}, \boldsymbol{\tau}, \boldsymbol{\Psi}, G)$ is the multivariate normal distribution

$$\mathcal{N}_p\left(\left[\left(\sum_{i=1}^{n} \tau_i\right)\boldsymbol{\Theta} + \boldsymbol{\Theta}_\mu\right]^{-1} \boldsymbol{\Theta}\left(\sum_{i=1}^{n} \tau_i \mathbf{Y}_i\right), \left[\left(\sum_{i=1}^{n} \tau_i\right)\boldsymbol{\Theta} + \boldsymbol{\Theta}_\mu\right]^{-1}\right) \tag{17}$$

where $\boldsymbol{\Theta}_\mu = \boldsymbol{\mathcal{I}}_p/\sigma_\mu$ and, again, $\boldsymbol{\Theta} = \boldsymbol{\Psi}^{-1}$. To draw $\boldsymbol{\mu}$ using this conditional distribution we must invert the $p \times p$ matrix $\left(\sum_{i=1}^{n} \tau_i\right)\boldsymbol{\Theta} + \boldsymbol{\Theta}_\mu$, a potentially computationally expensive procedure. For practical applications, we thus simply set

$$\boldsymbol{\mu} = \frac{\sum_{i=1}^{n} \tau_i \mathbf{Y}_i}{\sum_{i=1}^{n} \tau_i} \tag{18}$$

instead of drawing from the conditional distribution in (17). We provide theoretical and numerical justifications for this alternative in Appendix 7.

Algorithm 2 (Classical t)**.** *Starting with a decomposable graph G_0, and initial values $\boldsymbol{\mu}_0$ and $\boldsymbol{\tau}_0$, repeat the following steps for $t = 0, 1, 2, \ldots$:*
(i) Jointly draw a new graph G_{t+1} and a new matrix $\boldsymbol{\Theta}_{t+1}$ as follows:

(a) Draw G_{t+1} as in Algorithm 1, but using the ratio in (12).

(b) Conditional on $(\mathbf{Y}, G_{t+1}, \boldsymbol{\tau}_t, \boldsymbol{\mu}_t)$, sample $\boldsymbol{\Theta}_{t+1}$ by drawing $\boldsymbol{\Psi}_{t+1}$ from (14) and inverting it using (16).

(ii) Conditional on $(\mathbf{Y}, G_{t+1}, \boldsymbol{\Psi}_{t+1})$, sample the new independent components of the vector $\boldsymbol{\tau}_{t+1} = (\tau_{t+1,1}, \ldots, \tau_{t+1,n})$ from (15).
(iii) Set $\boldsymbol{\mu}_{t+1}$ to the value in (18).

In practice we hope to improve on the estimate of $P(G \,|\, \mathbf{Y})$ that we would obtain from the normal model. If we start with a "good" estimate of $\boldsymbol{\tau}$ as given by the *tlasso* of Finegold and Drton (2011), we may be able to make considerable improvement over the normal model without sampling $\boldsymbol{\tau}$ after every edge draw. In our later simulations, we thus draw $\boldsymbol{\tau}$ only every $k > 1$ draws of $(G, \boldsymbol{\Theta})$, which does not affect the validity of the sampler. Note also that the $k-1$ intermediate iterations do not involve $\boldsymbol{\Psi}$ (or its inverse $\boldsymbol{\Theta}$).

3.3 Bayesian Inference With Alternative t-Distributions

For the alternative t-model, we have the same factorization as in (9) except that now $\boldsymbol{\tau}_i$ is a p-vector, and the model for the observations is given by

$$\begin{aligned}(\mathbf{Y}_i \,|\, \boldsymbol{\tau}_i, \boldsymbol{\Psi}, \boldsymbol{\mu}) &\sim \mathcal{N}_p(\boldsymbol{\mu}, \mathrm{diag}(1/\sqrt{\boldsymbol{\tau}_i}) \cdot \boldsymbol{\Psi} \cdot \mathrm{diag}(1/\sqrt{\boldsymbol{\tau}_i})), \\ (\tau_{ij} \,|\, \nu) &\sim \Gamma(\nu/2, \nu/2), \quad j = 1, \dots, p,\end{aligned} \tag{19}$$

with $\tau_{i1}, \dots, \tau_{ip}$ independent given ν. For the Gibbs sampler, we cannot draw the matrix $\boldsymbol{\tau} = (\tau_{ij})$ given $\mathbf{Y}, \boldsymbol{\Theta}, G, \boldsymbol{\mu}$ directly, but we can draw τ_{ij} given $\boldsymbol{\tau}_{i,\setminus j}, \mathbf{Y}, \boldsymbol{\Theta}, G, \boldsymbol{\mu}$. Here, $\setminus j$ denotes the complement $\{1, \dots, p\} \setminus \{j\}$. The conditional density is

$$f(\tau_{ij} \,|\, \boldsymbol{\tau}_{i,\setminus j}, \mathbf{Y}) = C(\alpha, \beta, \gamma) \cdot \tau_{ij}^{\alpha-1} \exp\left\{-\tau_{ij}\beta - \sqrt{\tau_{ij}}\gamma\right\} \tag{20}$$

with

$$\alpha = \frac{\nu+1}{2}, \qquad \beta = \frac{\nu + (Y_{ij} - \mu_j)^2 \theta_{jj}}{2}, \qquad \gamma = (Y_{ij} - \mu_j)\boldsymbol{\Theta}_{j,\setminus j}\mathbf{X}_{i,\setminus j},$$

and normalizing constant $C(\alpha, \beta, \gamma)$. The problem of sampling from this density also arose in the work of Finegold and Drton (2011), where the density appears in the context of a Markov chain Monte Carlo EM algorithm. We employ a rejection sampling scheme from Liu et al. (2013); see also Finegold and Drton (2011, Section 5.2). This leads to the following Gibbs sampler.

Algorithm 3 (Alternative t)**.** *Starting with a decomposable graph G_0, and initial values $\boldsymbol{\mu}_0$ and $\boldsymbol{\tau}_0$, repeat the following steps for $t = 0, 1, 2, \dots$:*
(i) Jointly draw a new graph G_{t+1} and a new matrix $\boldsymbol{\Theta}_{t+1}$ as in Algorithm 2.
(ii) For each observation $i = 1, \dots, n$, cycle through the variables $j = 1, \dots, p$ and draw τ_{ij} from its current full conditional in (20) to obtain a new matrix $\boldsymbol{\tau}_{t+1}$.
(iii) Set $\boldsymbol{\mu}_{t+1}$ to the value in (18), where $\boldsymbol{\tau}$ is now a vector and the multiplications and divisions are done component-wise.

This sampling scheme for the alternative model works well for moderate p ($p \approx 100$) and underlies our later simulations. The scheme becomes very computationally intensive, however, for large p, both in terms of the time to complete one iteration of step (ii) above and the number of iterations required to approach convergence of the Markov chain. It is conceivable that other strategies, such as using a Metropolis-Hastings step to sample from $P(\boldsymbol{\tau}|G, \mathbf{Y})$ directly, might perform better. However, we will not treat such alternative sampling schemes in the remainder of this paper, which is instead devoted to other models.

4 Dirichlet t-Models

We are faced with a trade-off between the classical and alternative models. If our goal is to identify pockets of contamination spread throughout a large data set, we certainly do not want to weight an entire observation via a single divisor as in the classical model. In the other extreme, with a different divisor for each variable, the alternative model proves to be computationally burdensome. Moreover, the alternative model has pairwise correlations bounded at a level that is somewhat restrictive for small degrees of freedom ν; see Finegold and Drton (2011). The approach we propose in this section interpolates between the two extremes and seems appealing in particular when there are batches of variables taking on extreme values, while the rest exhibit behavior consistent with a normal model.

If groups of variables are similarly contaminated (or otherwise extreme), we can share statistical strength and ease our computational burden by forming clusters of Gamma divisors for each observation. We solve this clustering problem via a Dirichlet Process (DP) prior on the vector of $\boldsymbol{\tau}$ divisors for each observation. This approach avoids fixing a number of clusters and truly interpolates between the classical and alternative case. Moreover, DPs tend to produce a single larger cluster; consider the 'rich-get-richer' formula in (21). In our context, this phenomonen has appeal as a single large cluster could group together uncorrupted observations. This said, other distributions for random partitions could be considered in place of the ones obtained by DPs.

4.1 Background on Dirichlet Processes

The Dirichlet process is a measure on measures introduced by Ferguson (1973). Let P_0 be a probability measure on a measurable space $(\boldsymbol{\Theta}, \mathcal{B})$, and $\alpha > 0$. We say that P is distributed according to a Dirichlet process with parameters α and P_0 if for any finite measurable partition $(A_1, \ldots, A_r)$ of $\boldsymbol{\Theta}$, the random vector $(P(A_1), \ldots, P(A_r))$ follows a Dirichlet distribution with parameters $(\alpha P_0(A_1), \ldots, \alpha P_0(A_r))$. We write $P \sim DP(\alpha, P_0)$. For more intuition about Dirichlet processes we refer to the reader to Sethuraman (1994) who describes the "stick-breaking construction" of the process.

The Dirichlet process possesses a clustering property due to the fact that if $P \sim DP(\alpha, P_0)$ then P is discrete with probability 1. This holds even if the base measure P_0 is continuous (Ferguson 1973). Let $\pi_1, \ldots, \pi_n$ be independent draws from a random measure $P \sim DP(\alpha, P_0)$. Then the conditional distribution of π_n given $\pi_{\setminus n}$ is a mixture, namely,

$$(\pi_n \,|\, \pi_{\setminus n}) \sim \frac{\alpha}{\alpha + n - 1} P_0(\pi_n) + \frac{1}{\alpha + n - 1} \sum_{j=1}^{n-1} \delta_{\pi_j}(\pi_n), \qquad (21)$$

where δ_{π_j} denotes a point mass at π_j. Hence, each new draw has a positive probability of assuming the same value as a previous draw, and this probability increases with each new draw. The choice of α greatly influences the number of expected clusters, with larger values leading to more clusters. New observations taking on the same values as

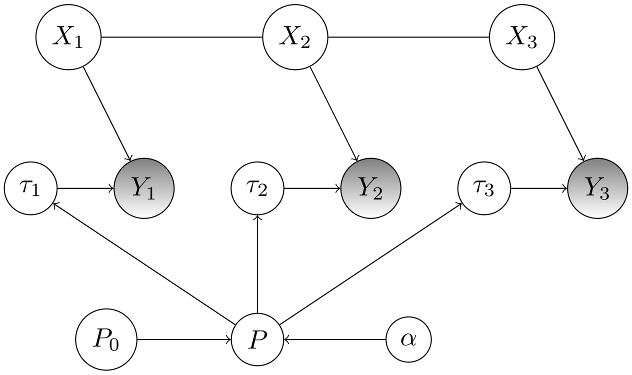

Figure 1: Representation of the process generating a t^{α}-random vector $\mathbf{Y}$ from a latent normal random vector $\mathbf{X}$ and an independent Dirichlet Gamma random vector $\boldsymbol{\tau}$. The missing undirected edge between X_1 and X_3 indicates a conditional independence. Directed arrows illustrate the functional relationship among $\mathbf{X}$, $\boldsymbol{\tau}$, and $\mathbf{Y}$.

existing ones in (21) gives an intuitive explanation to the phenomenon that Dirichlet processes often produce a small number of large clusters. This can be unsuitable for generic clustering applications but is, in fact, appealing for the robustification problem we consider. Here, we might often expect one large cluster that corresponds to uncontaminated (high-quality) observations.

4.2 Dirichlet t-Model

Applying Dirichlet processes in the t-distribution context yields the following construction, illustrated in Figure 1.

Definition 1. *Let P_0 be the $\Gamma(\nu/2, \nu/2)$ distribution and let $P \sim DP(\alpha, P_0)$. For $j = 1, \ldots, p$, let $\tau_j \sim P$ be independent of each other given P. We then say that the random vector $\boldsymbol{\tau} \in \mathbb{R}^p$ follows a Dirichlet Gamma distribution; in symbols $\boldsymbol{\tau} \sim D\Gamma_p(\alpha, \nu)$. If the random vectors $\mathbf{X} \sim \mathcal{N}_p(\mathbf{0}, \boldsymbol{\Psi})$ and $\boldsymbol{\tau} \sim D\Gamma_p(\alpha, \nu)$ are independent, then we say that $\mathbf{Y} \in \mathbb{R}^p$ with coordinates $Y_j = \mu_j + X_j/\sqrt{\tau_j}$ follows a Dirichlet t-distribution; in symbols $\mathbf{Y} \sim t^{\alpha}_{p,\nu}(\boldsymbol{\mu}, \boldsymbol{\Psi})$.*

The family of Dirichlet t-distributions includes the previous two models as extreme cases. When $\alpha \to 0$, we will have one cluster, giving us the classical t-distribution. When $\alpha \to \infty$ we will have p clusters, giving us the alternative t-distribution.

Unlike in the alternative model, there is no upper bound on the correlations between two variables *within* a cluster. For *any* two variables Y_j and Y_k, the marginal covariance is

$$\psi_{jk}\left[\frac{1}{\alpha+1}\frac{\nu}{\nu-2} + \frac{\alpha}{\alpha+1}\frac{\nu\Gamma((\nu-1)/2)^2}{2\Gamma(\nu/2)^2}\right]. \tag{22}$$

Note that $1/(\alpha+1)$ is the probability that any two variables will be in the same τ cluster. As $\alpha \to 0$ we obtain a maximum covariance of $\psi_{jk} \cdot \nu/(\nu-2)$ and a maximum correlation of 1.

The alternative t is more flexible than the classical t, allowing us to downweight contaminated components of one high-dimensional observation, but consider the case where a number of components are contaminated by the same mechanism. Since the divisors in the alternative model are independent for each component, this type of phenomenon is poorly explained. The simulated bivariate densities in Figure 2 demonstrate the potential usefulness of the Dirichlet t. Large absolute values in both variables are plausible in the Dirichlet case, even when the concentration matrix is the identity.

When considering a Dirichlet t-model for the n independent observations in a sample $\mathbf{Y}_1, \dots, \mathbf{Y}_n$, then

$$(\mathbf{Y}_i \mid \boldsymbol{\tau}_i, \boldsymbol{\Psi}, \boldsymbol{\mu}) \sim \mathcal{N}_p(\boldsymbol{\mu}, \operatorname{diag}(1/\sqrt{\boldsymbol{\tau}_i}) \cdot \boldsymbol{\Psi} \cdot \operatorname{diag}(1/\sqrt{\boldsymbol{\tau}_i})),$$

as in (19). However, the n independent vectors of Gamma divisors $\boldsymbol{\tau}_i = (\tau_{i1}, \dots, \tau_{ip})$ are now distributed as

$$(\tau_{ij} \mid P_i) \overset{\text{i.i.d.}}{\sim} P_i, \quad j = 1, \dots, p, \qquad\qquad (P_i \mid \nu) \sim DP(\alpha, P_0).$$

We emphasize that $P_1, \dots, P_n$ are independent draws from the Dirichlet process with $P_0 = \Gamma(\nu/2, \nu/2)$ so that $\mathbf{Y}_1, \dots, \mathbf{Y}_n$ are independent.

Dirichlet processes are often used in mixture modeling (Antoniak 1974). In that context, n values are generated independently from a distribution that follows a Dirichlet process and these values are then associated with n observations. In contrast, we here draw p values for the coordinates of a single multivariate observation. The relevant conditional distributions are similar to those given in Escobar and West (1995) but include terms that reflect that dependence among the p coordinates of an observation.

4.3 Gibbs Sampling for the Dirichlet t-Model

For Gibbs sampling we need the following full conditional (derived in Appendix 7). For notational simplicity we consider $\mathbf{Y}$ and $\boldsymbol{\tau}$ to be p-vectors representing a single observation:

$$(\tau_j \mid \boldsymbol{\tau}_{\setminus j}, \mathbf{Y}, \boldsymbol{\Theta}) \sim q_0 P_j(\tau_j) + \sum_{j' \neq j} q_{j'} \delta_{\tau_{j'}}(\tau_j). \tag{23}$$

This mixture distribution involves point masses, denoted $\delta_{\tau_k}(\tau_j)$ when supported at τ_k, and the distribution $P_j(\tau_j)$, which is the conditional distribution of τ_j given $(\boldsymbol{\tau}_{\setminus j}, \mathbf{Y}, \boldsymbol{\Theta})$ from the alternative t-model. The mixture weights for the point masses are denoted $q_{j'}$ and are proportional to the conditional density of $(Y_j \mid \boldsymbol{\Theta}, \mathbf{Y}_{\setminus j}, \boldsymbol{\tau}_{\setminus j}, \tau_j = \tau_{j'})$ evaluated at y_j. This density is that of a normal distribution with mean $\mu_c/\sqrt{\tau_{j'}}$ and variance $\sigma_c^2/\tau_{j'}$ evaluated at $y_j - \mu_j$. We denote the density as $f_{\mathcal{N}}(y_j - \mu_j; \mu_c/\sqrt{\tau_{j'}}, \sigma_c^2/\tau_{j'})$. Finally, the remaining mixture weight q_0 is proportional to α times the conditional

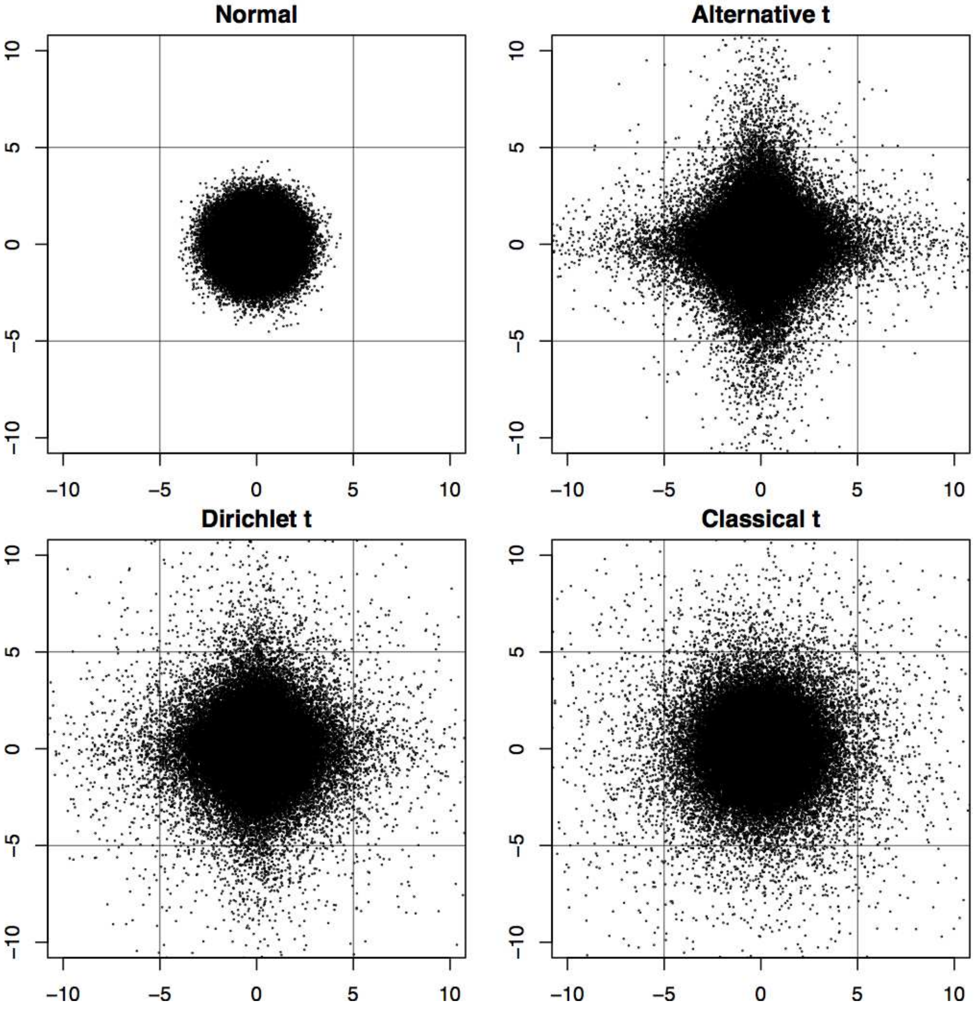

Figure 2: We simulate 100,000 draws from four bivariate distributions: the normal $\mathcal{N}_2(\mathbf{0}, \boldsymbol{\mathcal{I}}_2)$ distribution, the alternative $t^*_{2,3}(\mathbf{0}, \boldsymbol{\mathcal{I}}_2)$ distribution, the Dirichlet $t^{\alpha=1}_{2,3}(\mathbf{0}, \boldsymbol{\mathcal{I}}_2)$ distribution, and the classical $t_{2,3}(\mathbf{0}, \boldsymbol{\mathcal{I}}_2)$ distribution. Consider the four corners of each plot, representing the probability of large absolute values in both variables. The alternative t distribution provides less support for these "joint outliers" than the Dirichlet or classical t.

density of $(Y_j \,|\, \mathbf{\Theta}, \mathbf{Y}_{\setminus j}, \boldsymbol{\tau}_{\setminus_j})$ evaluated at y_j, where $\tau_j \sim P_0$. This density is that of a noncentral t-distribution with degrees of freedom ν and noncentrality parameter μ_c/σ_c, where μ_c and σ_c are the conditional mean and standard deviation of $(X_j \,|\, \mathbf{X}_{\setminus j})$. We denote the density as $f_T(y_j - \mu_j; \mu_c/\sigma_c, \nu)/\sigma_c$.

Now define a vector $\boldsymbol{z} \in \mathbb{R}^p$ of cluster indicators by setting $z_j = k$ if τ_j belongs to the k^{th} cluster. In our setting, all τ_j in the k^{th} cluster assume the same value, η_k, and thus $\boldsymbol{\tau}$ is a function of $\boldsymbol{z}$ and the vector of cluster values $\boldsymbol{\eta}$. Hence, we may rewrite (23) as

$$(\tau_j \,|\, \boldsymbol{\tau}_{\setminus j}, \mathbf{Y}, \mathbf{\Theta}) \sim q_0 P_j(\tau_j) + \sum_{k=1}^{K} q_k \delta_{\eta_k}(\tau_j), \tag{24}$$

where K denotes the number of clusters, and q_k is proportional to

$$n_k^{(j)} \cdot f_{\mathcal{N}}(y_j - \mu_j; \mu_c/\sqrt{\eta_k}, \sigma_c^2/\eta_k)$$

with $n_k^{(j)} = |\{j' \neq j \,:\, z_{j'} = k\}|$. Rewriting (24) using the conditional cluster assignments gives

$$(z_j \,|\, \boldsymbol{z}_{\setminus j}, \boldsymbol{\eta}, \mathbf{Y}, \mathbf{\Theta}) \sim q_0 \delta_{z_{new}}(z_j) + \sum_{k=1}^{K} q_k \delta_k(z_j), \tag{25}$$

where $z_{new} = K + 1$ unless $n_{z_j}^{(j)} = 0$ in which case $z_{new} = z_j$.

The conditional in (25) describes the assignment of one node to a cluster given all the other cluster assignments and cluster values. We can also derive the conditional distribution of one cluster value given all the other cluster values and all the cluster assignments. Let $(k) := \{j : z_j = k\}$ and $n_k = |(k)|$. The conditional density (derived in Appendix 7) is

$$f(\eta_k \,|\, \boldsymbol{\eta}_{\setminus k}, \mathbf{Y}, \mathbf{\Theta}, \boldsymbol{z}) = C(\alpha, \beta, \gamma) \cdot \eta_k^{\alpha - 1} \exp\{-\eta_k \beta - \sqrt{\eta_k}\gamma\} \tag{26}$$

with

$$\alpha = \frac{\nu + n_k}{2}, \qquad \beta = \frac{\nu + tr(\mathbf{\Theta}_{(k)(k)} \mathbf{Y}_{(k)} \mathbf{Y}_{(k)}^T)}{2}, \qquad \gamma = tr(\mathbf{\Theta}_{(k)\setminus(k)} \mathbf{X}_{\setminus(k)} \mathbf{Y}_{(k)}^T).$$

The density being similar to (20), sampling can be performed using the same rejection sampling scheme. When the number of clusters is small relative to p, cycling through the clusters and drawing values for the whole cluster is much faster than cycling through all p nodes and assigning each to a cluster (and drawing values when new clusters are formed).

The Dirichlet Process parameter α plays a key role in determining the number of clusters, and it is beneficial to add another level of hierarchy and place a prior on α. Following Escobar and West (1995) who treat Dirichlet process mixture models, we consider a $\Gamma(a, b)$ prior on α. In practice we choose a and b to give low prior mean to

α, which leads to fewer clusters and easier computation, but allows for more clusters as the data requires. The required conditionals for the Gibbs sampler are based on a generalization of Escobar and West (1995); details can be found in Appendix 7.

Now suppose we observe n independent random vectors $\mathbf{Y}_1, \ldots, \mathbf{Y}_n \in \mathbb{R}^p$ that follow a $t^{\alpha}_{p,\nu}(\boldsymbol{\mu}, \boldsymbol{\Psi})$ distribution. Once again, let $\mathbf{Y}$ and $\boldsymbol{\tau}$ be the associated matrices of observations and divisors. For small α, i.e., few expected clusters, we can create a sampler as follows. Let k_i be the number of clusters for the i^{th} observation. The state space consists of the values for $(G, \boldsymbol{\Theta}, \boldsymbol{z}, \boldsymbol{\eta})$ where $\boldsymbol{z} = \{z_{ij}\}$ is now an $n \times p$ matrix and $\boldsymbol{\eta}$ an array collecting n vectors of length $k_1, \ldots, k_n$. Following Teh et al. (2006), we propose the following Gibbs sampler.

Algorithm 4 (Dirichlet t)**.** *Starting with a decomposable graph G_0, and initial values $\boldsymbol{\mu}_0$, $\boldsymbol{z}_0$, α_0, and $\boldsymbol{\eta}_0$, repeat the following steps for $t = 0, 1, 2, \ldots$:*
(i) Jointly draw a new graph G_{t+1} and a new matrix $\boldsymbol{\Theta}_{t+1}$ as in Algorithm 2.
(ii) For each observation $i = 1, \ldots, n$, cycle through the variables $j = 1, \ldots, p$ and draw z_{ij} from the conditional given in (25). If $z_{ij} = z_{new}$ assign to this new cluster a value $\eta_{iz_{new}}$ by sampling from $P_j(\tau_j)$ in (23). This results in a new matrix $\boldsymbol{z}_{t+1}$.
(iii) For each observation $i = 1, \ldots, n$, cycle through the clusters $k = 1, \ldots, K_i$ and draw η_{ik} using (26). This results in a new array $\boldsymbol{\eta}_{t+1}$.
(iv) Assign $\boldsymbol{\mu}_{t+1}$ as in Algorithm 3.
(v) For each observation $i = 1, \ldots, n$, draw w_i from the conditional given in (36).
(vi) Draw α from the conditional given in (34).

In the algorithm we may repeat some steps more frequently than others. For instance, if we are able to quickly identify clusters representing significant deviations from normality, then we can perform the third step more frequently than the computationally expensive reclustering step. For initial values, we use the *tlasso* of Finegold and Drton (2011) to estimate $\boldsymbol{\tau}$, which means we have one cluster for each observation.

5 Simulations

5.1 AR1 With p=25

To illustrate the behaviour of the different Bayesian methods, we first present simulations for graphs with 25 nodes, for which we run the Markov chain Monte Carlo samplers for 10,000 iterations per possible edge, as suggested in Jones et al. (2005). We choose a graph for an autoregressive process of order one, that is, the nodes form a chain and the corresponding precision matrix $\boldsymbol{\Theta}$ is tri-diagonal. We forego simulating random draws of $\boldsymbol{\Theta}$ for a clear distinction between true positives and negatives. Instead, we set the non-zero off-diagonal elements of $\boldsymbol{\Theta}$ to -1 and the diagonal elements to 3 (except the first and last, which are set to 2). Unless otherwise noted, we fix the degrees of freedom $\nu = 3$, the graph prior parameter $d = 0.05$, recall (3), and the hyperparameter $\delta = 1$. It is not desirable, however, to have exactly the same priors in the normal and t-models. With the most extreme observations downweighted, the entries of the matrix $\boldsymbol{S}_{\boldsymbol{\tau}\mathbf{YY}}$ from the t-model tend to be smaller in magnitude than those of the sample covariance matrix $\boldsymbol{S}$, and, in our experience, the same hyperparameter matrix $\boldsymbol{\Phi}$ then leads to larger graphs for the t-case. To get graphs of comparable size, we choose $\boldsymbol{\Phi} = \boldsymbol{\mathcal{I}}_p/5$ for the normal model and $\boldsymbol{\Phi} = \boldsymbol{\mathcal{I}}_p/10$ for t-models.

We first simulate n independent normal observations from $\mathcal{N}_p(\mathbf{0}, \boldsymbol{\Theta}^{-1})$. In order to illustrate the effects on inference of dependence structures, we assume the mean to be known and run five different estimation methods:

(a) The normal procedure (Section 2).

(b) The normal procedure using the maximum likelihood estimate $\boldsymbol{S}_{\hat{\boldsymbol{\tau}}\mathbf{YY}}$ from the classical $t_{p,3}$-model as the sufficient statistic instead of $\boldsymbol{S}$.

(c) The classical $t_{p,3}$ procedure (Section 3.2), drawing the matrix $\boldsymbol{\tau}$ once every 10 edge proposals.

(d) The Dirichlet $t^{\alpha}_{p,3}$ procedure (Section 4.2) with a $\Gamma(1,1)$ prior on α. We draw new cluster identifiers $\boldsymbol{z}$ for every 20 draws of $\boldsymbol{\eta}$, which in turn is drawn once every 10 edge proposals.

(e) The alternative $t^{*}_{p,3}$ procedure (Section 3.3), drawing the matrix $\boldsymbol{\tau}$ once every 10 edge proposals.

Assuming known means only favors normal procedures for which estimation of the mean from heavy-tailed data is problematic in itself. For each method, we perform 3 million edge proposals. We repeat the process 50 times, each time recording the posterior probability $P(e_{jk} = 1 \,|\, \mathbf{Y})$, that is, the probability of edge $\{j, k\}$ being in the true edge set. If $P(e_{jk} = 1 \,|\, \mathbf{Y}) > \epsilon$ for some threshold ϵ, we consider it a "positive". We let ϵ range from 0 to 1 and record the number of true and false positives in all 50 simulations. We then compare the true positive rate to the false positive rate at each threshold and draw the resulting receiver operating characteristic (ROC) curve. This entire process is repeated for data generated from a $t_{p,3}(\mathbf{0}, \boldsymbol{\Theta}^{-1})$ and a $t^{*}_{p,3}(\mathbf{0}, \boldsymbol{\Theta}^{-1})$ distribution.

The simulation results are summarized in Figure 3, which shows that the more flexible models indeed perform better when the data is generated from the more complicated model. With normal data, the t-models all perform similarly well and the normal model outperforms them only slightly. For classical t-data, the classical t-model performs significantly better than the normal model. The alternative model is clearly inferior to the classical model. The performance of the Dirichlet t-model, on the other hand, is barely distinguishable from that of the classical t-model. With a $\Gamma(1,1)$ prior for α, the Dirichlet method finds an average of 1.4 clusters per $\boldsymbol{\tau}$ vector, rendering it very similar to the classical model. The normal procedure with the robustified estimate $\boldsymbol{S}_{\hat{\boldsymbol{\tau}}\mathbf{YY}}$ performs better than the purely normal technique, but not as well as the classical t-model. In addition to the superior performance seen here, the fully Bayesian approach has, of course, the added benefit of a posterior distribution on $\boldsymbol{\tau}$. This can be useful to assess each observation's consistency with normality.

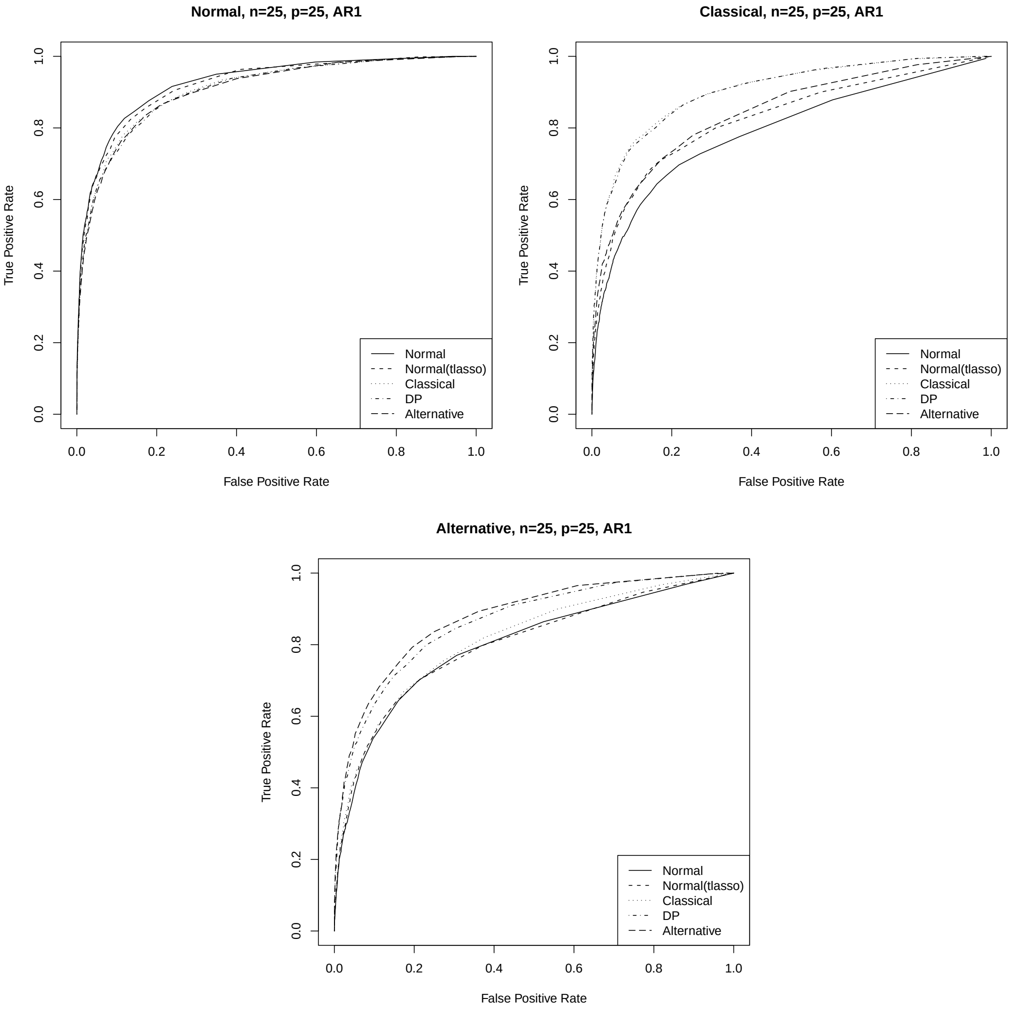

Normal, n=25, p=25, AR1

Classical, n=25, p=25, AR1

Alternative, n=25, p=25, AR1

Figure 3: ROC curves depicting the performances of the five methods for data generated from a $\mathcal{N}_{25}(\mathbf{0}, \mathbf{\Theta}^{-1})$ distribution, a $t_{25,3}(\mathbf{0}, \mathbf{\Theta}^{-1})$ distribution and a $t^*_{25,3}(\mathbf{0}, \mathbf{\Theta}^{-1})$ distribution.

For alternative t-data, the alternative t-method clearly outperforms its normal and classical t-analogues, which perform equally poorly. Only the Dirichlet t-model, which finds an average of 7.7 clusters per $\boldsymbol{\tau}$ vector, performs comparably to the alternative model. Its strong performance on both classical and alternative data suggests that the Dirichlet method is indeed an effective compromise between the two other t-distribution techniques.

For classical t-data, the processing times to fit the classical, the Dirichlet and the alternative t-model were on average $2.3N$, $3.6N$ and $4.5N$, respectively, where N is the processing time for the normal model. Based on use of 'R' (R Development Core Team 2010), the times are meant only to be rough estimates of actual computational complexity. Nevertheless, the comparison suggests that the Dirichlet approach adaptively produces statistically efficient estimates while using a run-time about halfway between that of the classical and alternative procedures. For alternative t-data, the Dirichlet model faces the added complexity of reclustering steps without much benefit from any clustering. Indeed, the average run time was $5N$ for the Dirichlet model compared to $3.8N$ for the alternative model. This said, we would not expect any real application to require as large a number of clusters as simulated alternative t-data.

5.2 Random Graphs With p=100

For a more challenging scenario, we consider $p = 100$ nodes and create the graph by forming 20 random cliques of size 2 to 5. For each clique, we pick nodes at random and form edges between all nodes in the clique. We draw the mean vector $\boldsymbol{\mu}$ as a p-vector of independent standard normals. We set the non-zero entries in Θ as before (but multiply the diagonal entries by a constant to ensure a minimum eigenvalue of at least 0.6). We then simulate $n = 100$ independent observations from a $\mathcal{N}_p(\mathbf{0}, \boldsymbol{\Theta}^{-1})$ distribution to create latent data X.

Next, we contaminate the data via an $n \times p$ matrix $\boldsymbol{\tau}$ that holds divisors for X, with the goal of creating contamination in many parts of many observations so that detecting outliers manually would be difficult. For each one of a total of 10 contaminations, we draw a Poisson number of rows and a Poisson number of columns (mean 10 for both). We then select uniformly at random a submatrix of $\boldsymbol{\tau}$ that has this given size and assign a single random value (uniform[0.01,0.2]) to the entries in the submatrix. The remaining entries of $\boldsymbol{\tau}$ are set to 1. The observations Y are created by setting $Y_{ij} = \mu_j + X_{ij}/\tau_{ij}$. This results on average in contamination in slightly less than one in ten elements of the latent data matrix.

We run the five algorithms from Section 5.1 under the settings described there, but with $\boldsymbol{\Phi} = \boldsymbol{\mathcal{I}}_p/5$ for the normal model and $\boldsymbol{\Phi} = \boldsymbol{\mathcal{I}}_p/20$ for t-models, to get graphs of comparable size. We run the samplers to obtain 2 million edge draws and for the t-models we sample $\boldsymbol{\tau}$ every 30 edge draws. The results for 25 repeats of the entire process are shown in Figure 4, which makes a clear case for the Dirichlet t-model. We remark that the 2 million draws do not seem enough for "convergence" of all Markov chains. Figure 5, which shows the number of edges in the estimated graph over the iterations

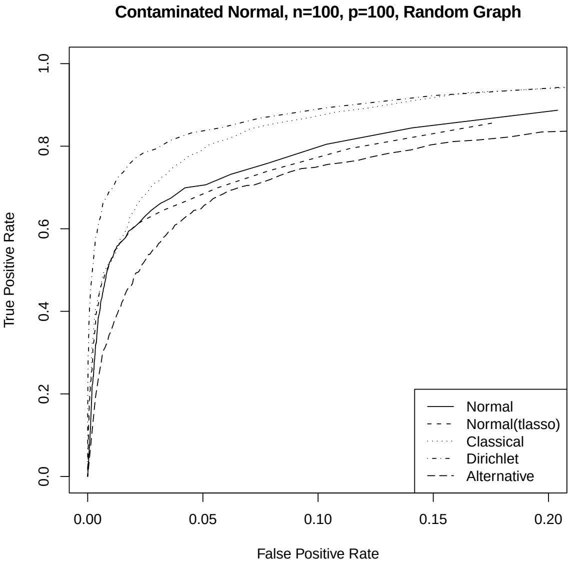

Figure 4: ROC curves depicting the performances of the five methods for data generated from a contaminated $\mathcal{N}_{100}(\mathbf{0}, \mathbf{\Theta}^{-1})$ distribution that is Markov to a random graph.

of the samplers, suggests that the alternative model may require much longer runs; the Dirichlet sampler fares better in this example. (The plot for the normal procedure (a) is omitted; it looks much like the one for the other normal procedure.)

6 Gene Expression Data

Gasch et al. (2000) present data from microarray experiments with yeast strands. To illustrate the workings of the proposed t-distribution models, we focus on 8 genes involved in galactose utilization; 136 experiments have data for all the 8 genes; compare also Finegold and Drton (2011). In 11 experiments, 4 of the genes have abnormally large negative expression values.

A first point we would like to make is that t-distribution models lead to downweighting of extreme values and that the Dirichlet t-model can achieve this by downweighting only the abnormal values but not entire observations, as desired. Figure 6 illustrates the downweighting via a plot of the posterior means of the Gamma divisors/weights τ_{ij}. It is obtained from 3 million iterations of our sampler for the Dirichlet $t^{\alpha}_{8,3}$ model with a $\Gamma(1, 1)$ prior on α.

The second point we would like to make is that the jointly extreme values indeed have an impact on inferences in graphical modeling. In Figure 7 we plot complete graphs whose edges are weighted by their (marginal) posterior probability under different models. These were obtained from 3 million iterations of each of the samplers.

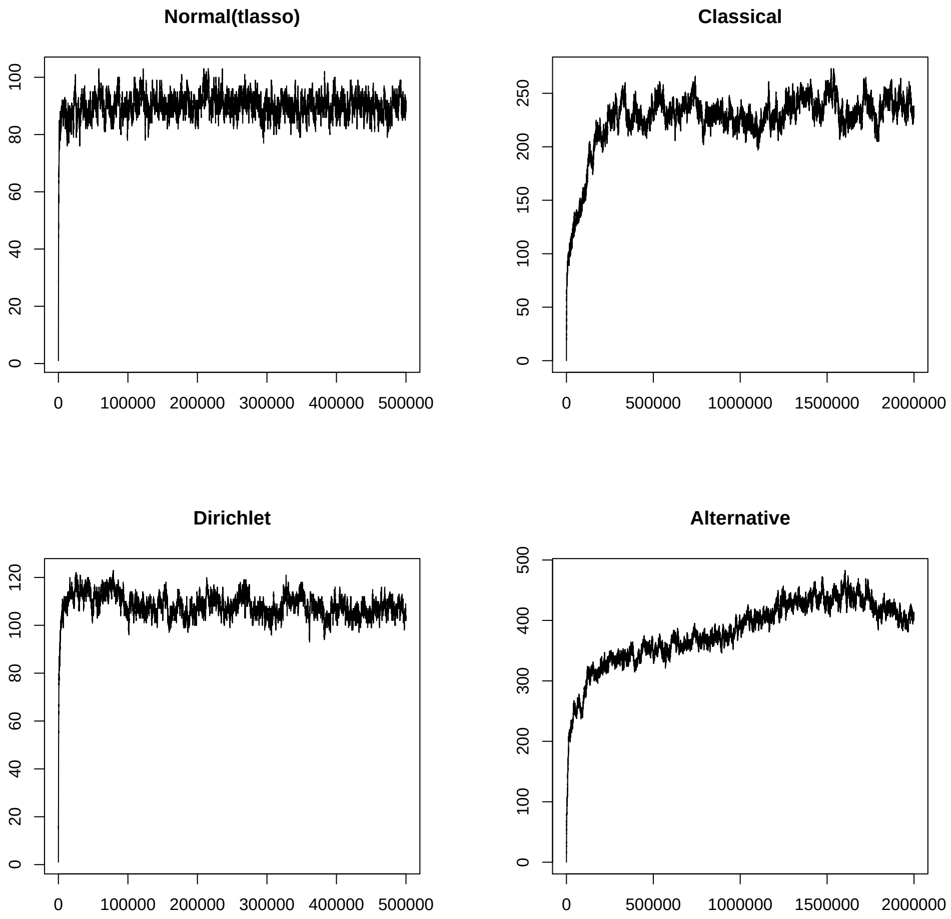

Figure 5: Number of edges in estimated graph plotted against iterations of the Gibbs sampler for models used in the contaminated normal simulations.

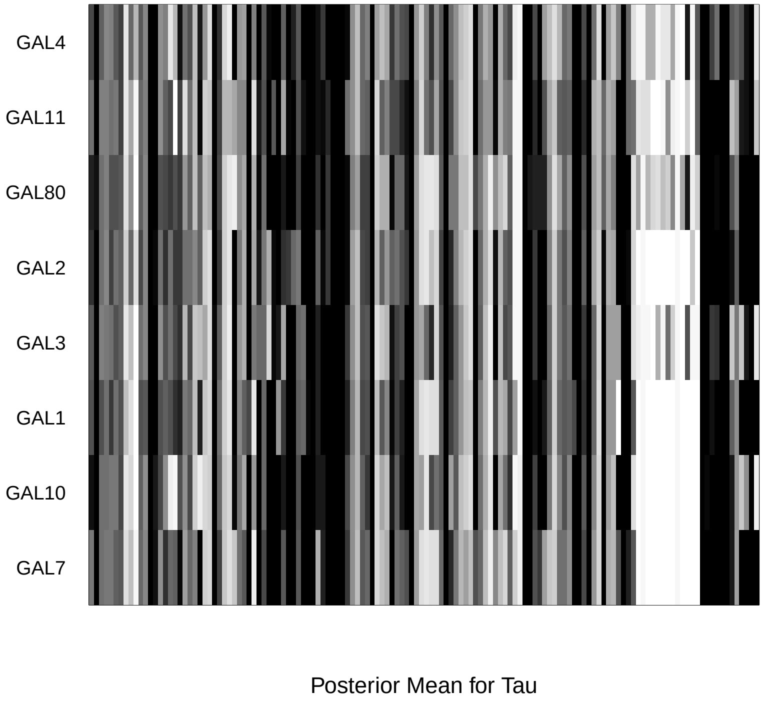

Figure 6: Gray-scale plot of posterior means of the weights τ_{ij}. The rows of the plot correspond to the variables indexed by j and the columns correspond to the observations indexed by i. Black indicates a value of 1 or larger; white indicates 0. The light blocks on the bottom right correspond to the "outliers" in the gene expression data from Section 6: GAL7, GAL10, GAL1, and GAL2 are the four genes with abnormally large values.

The edges that are dark grey in Figure 7 are common to all graphs with large posterior probability (according to our MCMC samplers). One observes that both t-models cast doubt on the edge between GAL7 and GAL1 that is common to many graphs with high posterior probability under the Gaussian model. The Gaussian posterior edge probability is about 0.45; the t-samplers estimate it to be no larger than 0.005. The two t-models give rather similar results, which suggests that there are few extreme observations apart from those in the mentioned 11 experiments. This said, in the Dirichlet t-model, the posterior probability for an edge between GAL3 and GAL10 is, in absolute terms, slightly increased from about 0.03 to about 0.1.

Finally, to illustrate the ability of Dirichlet t-models to reweight individual groups of observations in individual experiments, we rerun our samplers on a larger data set obtained by adding the data for 92 genes, selected at random from those without missing data. We fit the models $t^{\alpha}_{100,3}$ for fixed $\alpha = \{1, 10, 100\}$ and also with a $\Gamma(1, 1)$ prior on α, and compare them to the fit of the classical t-model.

For $\alpha = 100$ the propensity to cluster is very weak with an average of 67 different

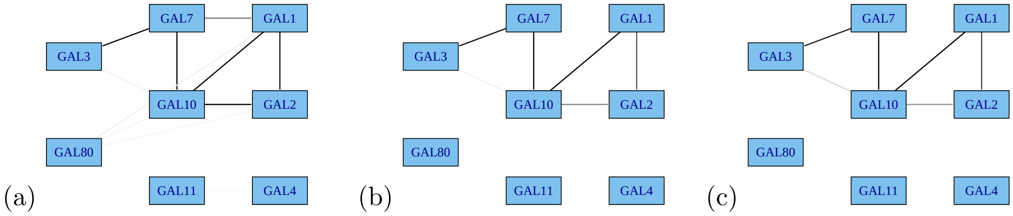

Figure 7: Complete graphs with edges weighted by their marginal posterior probability: (a) Gaussian model, (b) Classical $t_{8,3}$-model, (c) Dirichlet $t^{\alpha}_{8,3}$-model with $\Gamma(1,1)$ prior on α. Edges not visible have very low posterior probability.

clusters in each row of $\boldsymbol{\tau}$ in the final iteration—very similar in practice to the alternative t procedure. Nonetheless, the average $\boldsymbol{\tau}$ value for the 4 relevant genes in the 11 relevant experiments was 0.06 of the average value of the matrix. That is, as we let the Dirichlet t-model approach the alternative model, we achieve downweights of the suspected outliers even without the benefits of clustering. With $\alpha = 10$ the propensity to cluster is a bit stronger; the rows of $\boldsymbol{\tau}$ have an average of 20 different clusters in the final iteration. We achieve relative downweighting similar to the $\alpha = 100$ model (0.13 of the average). Despite 20 clusters per row, at least two of the outliers always share a cluster and in five of the experiments, at least three share a cluster. Letting $\alpha = 1$, we achieve much greater clustering (2.8 per row). The suspected outliers tend to cluster together and have an average value 0.13 of the average.

Putting a prior on α, we get a posterior mean of 0.07 for α, leading to only 1.4 clusters per row. Yet the outliers still tend to cluster together and are downweighted relative to the rest (0.18 of the average for the matrix). The τ values are also 0.03 of the average values for the entire outlier observations. That is, even with limited clustering, the Dirichlet t is able to downweight just the relevant components without downweighting the entire observation. In contrast, for the classical t, outliers are 0.76 of the average—so not much relative downweighting is achieved. The outliers, of course, must have the same τ value as the rest of the observation. In summary, the Dirichlet t with a prior on α appears to do a good job of creating just enough clusters to downweight the apparent outliers relative to the rest.

7 Discussion

We have extended Bayesian approaches to graphical Gaussian modeling using three variations of multivariate t-distributions. While these extensions all come at increased computational expense, they can have substantial statistical benefit. In particular, one obtains a posterior distribution for latent weights that measures uncertainty about potential outliers.

Our extensions to t-distributions are based on one particular Gaussian model, but many other variations have been treated in the literature. Some authors place a prior on the degrees of freedom parameter δ for the Hyper Inverse Wishart (HIW) prior distribution. In addition, one can introduce a prior on the edge density parameter d from (3). An alternative approach is to place a uniform prior on the size of the graph, and then a uniform prior on all graphs of the same size. We have chosen the scale matrix of the HIW prior to be $\boldsymbol{\Phi} = c\boldsymbol{\mathcal{I}}_p$ and treated fixed choices of c in our simulations. One could instead include a prior on c, or set $\boldsymbol{\Phi} = c\boldsymbol{A}$, where $\boldsymbol{A}$ is the sample covariance matrix, or an equicorrelated matrix with diagonal elements equal to 1 and off-diagonal elements equal to a common value ρ. Armstrong et al. (2009) consider all of these variations, including placing a prior on ρ. Finally, as mentioned in the introduction, there now exist more flexible versions of the HIW distribution as well as techniques for approximate computations for non-decomposable graphs. Incorporating these in the t-distribution context would be straightforward. For instance, the approximations of Atay-Kayis and Massam (2005) and Lenkoski and Dobra (2011) could be applied to compute the ratio in (12) when dealing with non-decomposable graphs.

As noted previously by many authors, for large p even the most likely graphs may have very small posterior probability, making it difficult and not necessarily very informative to identify the graph with highest posterior probability. In practice, the focus may thus often be on more modest goals, such as the posterior distribution of subgraphs on some subset of vertices, or even more simply, the marginal posterior probability that each edge is in the edge set E that we considered in the simulation study.

In the data from Section 6, a group of genes had extreme expression values in several observations. While the Dirichlet t-model did a good job identifying these clusters, it could potentially be worthwhile to share statistical strength by explicitly modeling the clustering of latent weights as similar across observations. This could be done by treating the p-vectors $\tau_1, \dots, \tau_n$ as draws from a Dirichlet process mixture model. Combined with the Dirichlet t-model, this would give a 'doubly Dirichlet' $\boldsymbol{\tau}$ matrix. That is, we will have $k \leq p$ distinct elements within each row (observation) and $l \leq n$ distinct rows. Inference in this model would be more involved than in the ordinary Dirichlet t-model we discussed, but the full conditionals necessary to devise a Gibbs sampler would be of similar type.

Finally, the emphasis of this paper has been on graphical models and the problem of graph recovery. However, the Dirichlet t-distribution we developed could also be of interest for other problems of multivariate statistics, and it would be interesting to assess possible merits of the framework in applications different from the one we treated.

Acknowledgments

This work was supported by the U.S. National Science Foundation under Grant No. DMS-0746265. Mathias Drton was also supported by an Alfred P. Sloan Fellowship.

The research was partially supported by the Singapore National Research Foundation under its International Research Centre @ Singapore Funding Initiative and administered by the IDM Programme Office through a grant for the joint Carnegie Mellon/Singapore Management University Living Analytics Research Centre.

This paper was invited by the Editor-in-Chief of Bayesian Analysis to be presented as the

2014 Best Bayesian Analysis Paper at the Twelfth World Meeting of International Society for Bayesian Analysis (ISBA2014), held in Cancún, Mexico, July 14-18, 2014, with invited discussions by Babak Shahbaba and François Caron

References

Antoniak, C. E. (1974). "Mixtures of Dirichlet processes with applications to Bayesian nonparametric problems." *Annals of Statistics*, 2: 1152–1174. 532, 548

Armstrong, H., Carter, C. K., Wong, K. F., and Kohn, R. (2009). "Bayesian covariance matrix estimation using a mixture of decomposable graphical models." *Statistics and Computing*, 19(3): 303–316. 524, 525, 543

Atay-Kayis, A. and Massam, H. (2005). "A Monte Carlo method for computing the marginal likelihood in nondecomposable Gaussian graphical models." *Biometrika*, 92(2): 317–335. 522, 543

Carvalho, C. and Scott, J. (2009). "Objective Bayesian model selection in Gaussian graphical models." *Biometrika*, 96(3): 1–16. 522, 524

Carvalho, C. M., Massam, H., and West, M. (2007). "Simulation of hyper-inverse Wishart distributions in graphical models." *Biometrika*, 94(3): 647–659. 527, 528

Cowell, R. G., Dawid, A. P., Lauritzen, S. L., and Spiegelhalter, D. J. (1999). *Probabilistic networks and expert systems*. Statistics for Engineering and Information Science. New York: Springer-Verlag. 525

Dawid, A. P. and Lauritzen, S. L. (1993). "Hyper-Markov laws in the statistical analysis of decomposable graphical models." *Annals of Statistics*, 21(3): 1272–1317. 522, 524, 525, 528

De Finetti, B. (1961). "The Bayesian approach to the rejection of outliers." In *Proceedings of the Fourth Berkeley Symposium on Probability and Statistics*, volume 1, 199–210. 522

Dellaportas, P., Giudici, P., and Roberts, G. (2003). "Bayesian inference for nondecomposable graphical Gaussian models." *Sankhyā*, 65(1): 43–55. 522

Dobra, A., Hans, C., Jones, B., Nevins, J. R., Yao, G., and West, M. (2004). "Sparse graphical models for exploring gene expression data." *Journal of Multivariate Analysis*, 90(1): 196–212. 522

Donnet, S. and Marin, J.-M. (2012). "An empirical Bayes procedure for the selection of Gaussian graphical models." *Statistics and Computing*, 22(5): 1113–1123. 524

Escobar, M. D. and West, M. (1995). "Bayesian density estimation and inference using mixtures." *Journal of the American Statistical Association*, 90(430): 577–588. 532, 534, 535, 548

Ferguson, T. S. (1973). "A Bayesian analysis of some nonparametric problems." *Annals of Statistics*, 1: 209–230. 530

Finegold, M. and Drton, M. (2011). "Robust graphical modeling with classical and alternative t-distributions." *Annals of Applied Statistics*, 5(2A): 1057–1080. 522, 528, 529, 530, 535, 539

Gasch, A. P., Spellman, P. T., Kao, C. M., Carmel-Harel, O., Eisen, M. B., Storz, G., Botstein, D., and Brown, P. O. (2000). "Genomic expression programs in the response of yeast cells to environmental changes." *Molecular Biology of the Cell*, 11: 4241–4257. 539

Giudici, P. and Green, P. J. (1999). "Decomposable graphical Gaussian model determination." *Biometrika*, 86(4): 785–801. 521, 525

Jones, B., Carvalho, C., Dobra, A., Hans, C., Carter, C., and West, M. (2005). "Experiments in stochastic computation for high-dimensional graphical models." *Statistical Science*, 20(4): 388–400. 522, 524, 535

Kotz, S. and Nadarajah, S. (2004). *Multivariate t distributions and their applications*. Cambridge: Cambridge University Press. 526

Lauritzen, S. L. (1996). *Graphical models*, volume 17 of *Oxford Statistical Science Series*. New York: The Clarendon Press Oxford University Press. Oxford Science Publications. 521, 523

Lenkoski, A. and Dobra, A. (2011). "Computational aspects related to inference in Gaussian graphical models with the G-Wishart prior." *Journal of Computational and Graphical Statistics*, 20(1): 140–157. 522, 543

Liu, C. and Rubin, D. B. (1995). "ML estimation of the t distribution using EM and its extensions, ECM and ECME." *Statistica Sinica*, 5(1): 19–39. 528

Liu, J. S. (2001). *Monte Carlo strategies in scientific computing*. Springer Series in Statistics. New York: Springer-Verlag. 527

Liu, Y., Wichura, M. J., and Drton, M. (2013). "Rejection sampling for an extended Gamma distribution." Unpublished manuscript. 529

R Development Core Team (2010). *R: A Language and Environment for Statistical Computing*. R Foundation for Statistical Computing, Vienna, Austria. ISBN 3-900051-07-0. 538

Rajaratnam, B., Massam, H., and Carvalho, C. M. (2008). "Flexible covariance estimation in graphical Gaussian models." *Annals of Statistics*, 36(6): 2818–2849. 522

Roverato, A. (2002). "Hyper inverse Wishart distribution for non-decomposable graphs and its application to Bayesian inference for Gaussian graphical models." *Scandinavian Journal of Statistics*, 29(3): 391–411. 522

Sethuraman, J. (1994). "A constructive definition of Dirichlet priors." *Statistica Sinica*, 4(2): 639–650. 530

Teh, Y. W., Jordan, M. I., Beal, M. J., and Blei, D. M. (2006). "Hierarchical Dirichlet processes." *Journal of the American Statistical Association*, 101(476): 1566–1581. 535

West, M. (1984). "Outlier models and prior distributions in Bayesian linear regression." *Journal of the Royal Statistical Society, Series B*, 46(3): 431–439. 522

Yuan, M. and Huang, J. (2009). "Regularized parameter estimation of high dimensional t distribution." *Journal of Statistical Planning and Inference*, 139: 2284–2292. 522

Appendix

A. Alternative Procedures for Drawing the Mean Vector $\boldsymbol{\mu}$

The parameters of the normal distribution in (17) involve the inverse of the sum of matrices $\sum_{i=1}^{n} \tau_i \boldsymbol{\Theta} + \boldsymbol{\Theta}_{\boldsymbol{\mu}}$, where $\boldsymbol{\Theta}_{\boldsymbol{\mu}} = \boldsymbol{\mathcal{I}}_p / \sigma_\mu$ is a multiple of the identity matrix. With rare exceptions, the hyperparameter σ_μ, a variance, is chosen large so as to make the prior distribution on $\boldsymbol{\mu}$ flat. In those cases, $\boldsymbol{\Theta}_{\boldsymbol{\mu}}$ is small compared to the typical values of $\sum_{i=1}^{n} \tau_i \boldsymbol{\Theta}$. Hence, little is lost by ignoring the term $\boldsymbol{\Theta}_{\boldsymbol{\mu}}$ in the matrix inversion, which leads to the distributional approximation

$$(\boldsymbol{\mu} \,|\, \mathbf{Y}, G, \boldsymbol{\tau}, \boldsymbol{\Theta}) \approx \mathcal{N}_p \left(\frac{1}{\sum_{i=1}^{n} \tau_i} \cdot \sum_{i=1}^{n} \tau_i \mathbf{Y}_i, \frac{1}{\sum_{i=1}^{n} \tau_i} \cdot \boldsymbol{\Theta}^{-1} \right). \tag{27}$$

This approximation still requires the completion step we have avoided to obtain $\boldsymbol{\Theta}^{-1} = \boldsymbol{\Psi}$. While this is not prohibitively expensive, we find that simply setting $\boldsymbol{\mu}$ equal to the mean of the distribution in (27) works well enough in practice – we call this "Robust Centering". To test this, we simulated classical t data from a chain graph with 25 nodes as described in Section 5. We ran four versions of the Dirichlet t algorithm (Algorithm 4) starting with the same seed: using naive centering (subtract off the sample mean for each variable and set $\boldsymbol{\mu} = \mathbf{0}$); Robust Centering; sampling from the approximate conditional in equation (27); and sampling from the exact conditional in (17). With σ_μ set to 100,000 we find virtually no difference between the estimated values of $\boldsymbol{\mu}$ from the last three procedures, but significant difference between those three and the first. The first procedure does a worse job of estimating $\boldsymbol{\mu}$ and, as a result, $\boldsymbol{\Theta}$. We conclude that Robust Centering is better than naive centering, but that virtually nothing is lost by failing to sample from the approximate or full conditionals.

B. Full Conditional for Latent Divisors in the Dirichlet t-Model

For notational convenience, let $z_j = 0$ if τ_j belongs to a new cluster and consider the case $j = p$. Let K be the number of distinct clusters containing elements other than τ_p.

We may then write

$$P(\tau_p \leq t \,|\, \boldsymbol{\tau}_{\backslash p}, \mathbf{Y}, \boldsymbol{\Theta}) = \sum_{k=0}^{K} P(\tau_p \leq t \,|\, \boldsymbol{\tau}_{\backslash p}, \mathbf{Y}, z_p = k) P(z_p = k \,|\, \boldsymbol{\tau}_{\backslash p}, \mathbf{Y}, \boldsymbol{\Theta}).$$

The conditional density of τ_p given $(\boldsymbol{\tau}_{\backslash p}, \mathbf{Y}, \boldsymbol{\Theta}, z = k)$ is trivially the point mass at η_k, the value assumed by all elements of $\boldsymbol{\tau}$ that belong to the k^{th} cluster. The conditional density of τ_p given $(\boldsymbol{\tau}_{\backslash p}, \mathbf{Y}, \boldsymbol{\Theta}, z = 0)$ is

$$\begin{aligned} f(\tau_p \,|\, \boldsymbol{\tau}_{\backslash p}, \mathbf{Y}, \boldsymbol{\Theta}, z = 0) &\propto f(\tau_p \,|\, \boldsymbol{\tau}_{\backslash p}, \boldsymbol{\Theta}, z = 0) f(\mathbf{Y} \,|\, \boldsymbol{\tau}, \boldsymbol{\Theta}, z = 0) \\ &= f(\tau_p \,|\, z = 0) f(\mathbf{Y} \,|\, \boldsymbol{\tau}, \boldsymbol{\Theta}) \\ &\propto f_\Gamma(\tau_p; \nu/2, \nu/2) f_\mathcal{N}(Y_p; \mu_c/\sqrt{\tau_p}, \sigma_c^2/\tau_p), \end{aligned} \tag{28}$$

where $f_\Gamma(\tau_p; \nu/2, \nu/2)$ is the density of a $\Gamma(\nu/2, \nu/2)$ distribution evaluated at τ_p. The distribution specified by (28) is the Gibbs sampling distribution from the alternative model in (20). Now,

$$\begin{aligned} P(z_p = 0 \,|\, \boldsymbol{\tau}_{\backslash p}, \mathbf{Y}, \boldsymbol{\Theta}) &\propto P(z_p = 0, Y_p \,|\, \mathbf{Y}_{\backslash p}, \boldsymbol{\tau}_{\backslash p}, \boldsymbol{\Theta}) \\ &= P(z_p = 0 \,|\, \boldsymbol{\tau}_{\backslash p}, \mathbf{Y}_{\backslash p}, \boldsymbol{\Theta}) P(Y_p \,|\, \mathbf{X}_{\backslash p}, \boldsymbol{\Theta}, z_p = 0) \\ &\propto \alpha P(Y_p \,|\, \mathbf{X}_{\backslash p}, \boldsymbol{\Theta}, z_p = 0). \end{aligned}$$

If $z_j = 0$ then X_j and τ_j are conditionally independent of $(\mathbf{Y}_{\backslash j}, \boldsymbol{\tau}_{\backslash j})$ and each other given $X_{\backslash j}$. Let μ_c and σ_c be the conditional mean and standard deviation of $(X_j \,|\, \mathbf{X}_{\backslash j})$. Therefore, given $\mathbf{X}_{\backslash j}$, the random variable Y_j/σ_c has the same distribution as

$$\frac{\mu_c/\sigma_c + Z}{\sqrt{\tau_j}}$$

for $Z \sim \mathcal{N}(0,1)$. We recognize the distribution as a noncentral t-distribution with degrees of freedom ν and noncentrality parameter μ_c/σ_c.

Similarly, for $k > 0$,

$$P(z_p = k \,|\, \boldsymbol{\tau}_{\backslash p}, \mathbf{Y}, \boldsymbol{\Theta}) \propto P(Y_p \,|\, \boldsymbol{\tau}_{\backslash p}, \mathbf{Y}_{\backslash p}, \boldsymbol{\Theta}, z_p = k).$$

Now, if $z_p = k$, then $Y_p = X_c/\sqrt{\tau_k}$ where $X_c \sim \mathcal{N}(\mu_c, \sigma_c)$. Therefore, the conditional distribution of Y_p given $\boldsymbol{\Theta}, \mathbf{Y}_{\backslash p}, \boldsymbol{\tau}_{\backslash_p}$, and $z_p = k$ is

$$f_Y(y) = f_{X_c}(\sqrt{\tau_k} y)\sqrt{\tau_k}.$$

Combining all the above elements gives the result stated in (25).

C. Full Conditional for Cluster Values in the Dirichlet t-Model

Define $(k) = \{j : z_j = k\}$ and $\backslash(k) = \{1, \ldots, p\} \setminus (k)$. First, note that the pair $(\mathbf{Y}_{(k)}, \eta_k)$ is conditionally independent of $\mathbf{Y}_{\backslash(k)}$ given $\mathbf{X}_{\backslash(k)}$. Hence,

$$f(\eta_k \,|\, \eta_{\backslash k}, \mathbf{Y}, \boldsymbol{\Theta}, z) = f(\eta_k \,|\, \mathbf{Y}_{(k)}, \mathbf{X}_{\backslash(k)}, z) \propto f(\eta_k, \mathbf{Y}_{(k)} \,|\, \mathbf{X}_{\backslash(k)}, z).$$

The last density is equal to

$$f(\eta_k \,|\, \mathbf{X}_{\setminus(k)}) f\left(\mathbf{Y}_{(k)} \,|\, \mathbf{X}_{\setminus(k)}, \eta_k, z\right) = f_\Gamma(\eta_k; \nu/2, \nu/2) \cdot f_{\mathcal{N}}\left(\mathbf{Y}_{(k)}; \frac{\mu_c}{\sqrt{\eta_k}}, \frac{\mathbf{\Sigma}_c}{\eta_k}\right) \tag{29}$$

where $\boldsymbol{\mu}_c$ and $\mathbf{\Sigma}_c$ are the conditional mean vector and covariance matrix of $\mathbf{X}_{(k)}$ given $\mathbf{X}_{\setminus(k)}$. By the well-known formulas for the inverse of a partitioned matrix, $\mathbf{\Theta}_{(k)(k)}$ is the inverse of $\mathbf{\Sigma}_c$, and $\boldsymbol{\mu}_c$ is equal to $\mathbf{\Theta}_{(k)(k)}\mathbf{\Theta}_{(k)\setminus(k)}\mathbf{X}_{\setminus(k)}$. The product in (29) is thus proportional to

$$\begin{aligned}&\eta_k^{\frac{\nu}{2}-1} \exp\left\{-\frac{\eta_k}{2}\nu\right\} |\eta_k \mathbf{\Theta}_{(k)(k)}|^{\frac{1}{2}} \exp\left\{-\frac{1}{2}\left(\mathbf{Y}_{(k)} - \frac{\boldsymbol{\mu}_c}{\sqrt{\eta_k}}\right)^T \eta_k \mathbf{\Theta}_{(k)(k)} \left(\mathbf{Y}_{(k)} - \frac{\boldsymbol{\mu}_c}{\sqrt{\eta_k}}\right)\right\} \\ &= \eta_k^{\frac{(\nu+|(k)|)}{2}-1} \exp\left\{-\frac{\eta_k}{2}\left[\nu + tr(\mathbf{\Theta}_{(k)(k)}\mathbf{Y}_{(k)}\mathbf{Y}_{(k)}^T)\right] - \sqrt{\eta_k} tr(\mathbf{\Theta}_{(k)\setminus(k)}\mathbf{X}_{\setminus(k)}\mathbf{Y}_{(k)}^T)\right\},\end{aligned}$$

which is the claim of (26). Note that when (k) is a singleton, we get the conditional distribution for the alternative model.

D. Inference for α in the Dirichlet t-Model

Let k denote the number of clusters. We have from Antoniak (1974) that, for $k = 1, \ldots, n$,

$$P(k \,|\, \alpha, n) = c_n(k) n! \alpha^k \frac{\Gamma(\alpha)}{\Gamma(\alpha + n)}, \tag{30}$$

where $c_n(k) = P(k \,|\, \alpha = 1, n)$. Posterior inference is simplified by the fact that α is conditionally independent of the observed data given the cluster assignments, leading to

$$P(\alpha \,|\, k, \pi, \mathbf{X}) = P(\alpha \,|\, k) \propto P(\alpha) P(k \,|\, \alpha). \tag{31}$$

That is, inference is based on the prior for α and a single observation from $P(k \,|\, \alpha, n)$.

Returning to our setting with an n-sample, let the vector $\mathbf{k} = (k_1, \ldots, k_n)$ comprise the numbers of clusters in the n observations. Then α is conditionally independent of $(\boldsymbol{\tau}, \mathbf{Y}, \mathbf{\Theta}, \boldsymbol{\mu}, G)$ given $\mathbf{k}$, and

$$P(\alpha \,|\, \mathbf{k}, \boldsymbol{\tau}, \mathbf{Y}, \mathbf{\Theta}, \boldsymbol{\mu}, G) \propto P(\alpha) P(\mathbf{k} \,|\, \alpha) = P(\alpha) \prod_{i=1}^n P(k_i \,|\, \alpha).$$

Let $\beta(\alpha, \beta)$ be the Beta function. Generalizing the results of Escobar and West (1995) to multiple observations k_i, we use the fact that

$$\frac{\Gamma(\alpha)}{\Gamma(\alpha + p)} = \frac{(\alpha + n)\beta(\alpha + 1, p)}{\alpha \Gamma(p)} \tag{32}$$

to obtain that $P(\alpha \,|\, \mathbf{k})$ is proportional to

$$P(\alpha)\alpha^{\sum k_i - n}(\alpha+p)^n \int_0^1 w_1^{\alpha}(1-w_1)^{p-1}dw_1 \times \cdots \times \int_0^1 w_n^{\alpha}(1-w_n)^{p-1}dw_n. \qquad (33)$$

Hence, we may view $P(\alpha \,|\, \mathbf{k})$ as a marginal distribution of $P(\alpha, w_1, \ldots, w_n \,|\, \mathbf{k})$ where $0 < w_i < 1$ are random variables that are conditionally independent of each other given α. Writing $\mathbf{w} = (w_1, \ldots, w_n)$, we consider the conditional distribution

$$P(\alpha \,|\, \mathbf{w}, \mathbf{k}) \propto \alpha^{a+\sum_{i=1}^n k_i - n - 1}(\alpha+p)^n \exp\Bigg\{ -\alpha\Bigg(b - \sum_{i=1}^n \log w_i\Bigg)\Bigg\}.$$

Expanding $(\alpha+p)^n$ gives a mixture of $n+1$ Gamma-distributions, namely,

$$(\alpha \,|\, \mathbf{w}, \mathbf{k}) \sim \sum_{j=0}^n \pi_j \Gamma\Bigg(a + \sum_{i=1}^n k_i - j, b - \sum_{i=1}^n \log w_i\Bigg) \qquad (34)$$

with

$$\pi_j \propto \binom{n}{j} p^j \left(b - \sum_{i=1}^n \log w_i\right)^j \Gamma\Bigg(a + \sum_{i=1}^n k_i - j\Bigg). \qquad (35)$$

The w_i being conditionally independent given α and $\mathbf{k}$, it holds that

$$(w_i \,|\, \alpha, \mathbf{k}, \mathbf{w}_{\setminus i}) \sim \beta(\alpha+1, p). \qquad (36)$$